Analytical Biochemistry 636 (2022) 114433

Contents lists available at ScienceDirect

Analytical Biochemistry

journal homepage: www.elsevier.com/locate/yabio

Research of exosome in bone metastasis through dual aptamer recognition based entropy-driven amplification

Chengxiang Yu [a,1], Lei Li [b,1], Lehong Liu [a], Zhongping Wang [a], Jianhua Zhu [b,*]

[a] The Third Surgical Department, Chongqing Sanbo Changan Hospital, No. 65, Jianxindong Road, Jiangbei District, Chongqing, 400700, China
[b] Spinal Surgery Department, Chongqing Ninth People's Hospital, No. 69, Jialing Village, Beibei District, Chongqing, 400700, China

ARTICLE INFO

Keywords:
Exosome
Entropy-driven amplification
Bone metastasis
Breast cancer

ABSTRACT

Sensitive and accurate detection of exosome will greatly facilitate the early diagnosis of diverse diseases, such as cancers. Herein, a novel dual aptamer recognition based entropy-driven amplification was established for accurate analysis of exosomes. There are two main procedures in the proposed biosensor, including dual aptamer based recognition of exosome and entropy-driven catalytic system based signal recycling. In the recognition process, designed SMBs-S1 probe and S2–S4 probe complex, containing a CD63 aptamer and an EpCAM aptamer, respectively, are utilized for cooperated identification of exosomes. S4 probe was then released from S2–S4 probe complex through chain replacement of S5. The released S4 probe triggers entropy-driven catalytic system based signal recycling and endow the method a superior sensitivity. Impressively, owing to the cooperated identification of CD63 and EpCAM protein, the method exhibited a superior specificity and stayed stable under the interference of free CD63 and/or EpCAM protein. We believe that the sensitive, accurate strategy will provide a powerful tool for multiple biomarkers analysis and related clinical applications.

1. Introduction

Bone metastasis of breast cancer makes patients suffer from pain, fractures, spinal cord compression, and hypercalcemia, and is almost incurable [1–4]. Although the mechanisms of bone metastasis in breast cancers have been studied intensively, novel specific target will be helpful to the development of new therapeutic strategy of breast cancer [5,6]. Exosomes are extracellular membrane vesicles with a diameter ranging from 30 to 200 nm, which mediate intercellular communication via transferring a wealth of nucleic acids and protein among cells under physiological and pathological conditions [7–9]. In recent years, accumulating reports confirmed that aberrant exosomes amounts and exosomal cargoes expression contribute to generating suitable microenvironments for engraftment and is becoming a valuable and promising biomarker for early diagnosis, treatment, and prognosis of cancers bone metastasis of breast cancer [10,11].

For efficient isolation and quantification of exosomes, a variety of novel methods have been proposed, such as ELISA (enzyme linked immunosorbent assay), NTA (nanoparticle tracking analysis), Western blot, and microarrays [12–17]. However, the requirement of complicated operation procedures, sophisticated instruments and extensive labor greatly limits their value in clinical and experimental application. Integrated with aptamer based signal convention, many signal amplification techniques have been utilized in exosome quantification for a more sensitive signal output, such as RCA (rolling circle amplification) [18–20], nuclease-assisted amplification [21,22], HCR (hybridization chain reaction) [23,24] and qRT-PCR (quantitative reverse transcription-polymerase). For example, ***Xianxian Zhao*** [22] proposed a CRISPR-Cas12 system based exosome detection method with CD63 protein on the surface of exosomal membrane as identification target. Through SMBs (streptavidin magnetic beads)-capture probe based separation and CRISPR-Cas12a based signal amplification, the method exhibited a detection range from 10^2 to 10^6 particles/μL. Although these amplified analytical strategies exhibited a high sensitivity and owned wide detection magnitudes, they inevitably require enzymes and thermocycling, which made them sensitive to surrounding experimental conditions, such as temperature, salinity, and pH, limiting their further applications. Furthermore, the fact that most of the former proposed exosome detection methods recognize one common surface protein, such as CD63 or EpCAM, causes false positive results when detecting exosome from complicated clinical samples due the inferences from free protein or cell debris. It is therefore highly desirable to develop reliable,

* Corresponding author. Spinal Surgery Department, Chongqing Ninth People's Hospital, No. 69, Jialing Village, Beibei District, Chongqing, China.
E-mail address: zhujianhua700@126.com (J. Zhu).
[1] Contributed Equally.

https://doi.org/10.1016/j.ab.2021.114433
Received 1 September 2021; Received in revised form 19 October 2021; Accepted 21 October 2021
Available online 25 October 2021
0003-2697/© 2021 Elsevier Inc. All rights reserved.

enzyme-free and accurate strategies for exosome isolation and quantification.

Herein, we developed a dual aptamer recognition based entropy-driven amplification strategy for accurate and sensitive qualification of exosomes in an enzyme-free way. There are two steps in the whole sensing system, including i) magnet based isolation of exosome and removal of supernatant and ii) entropy-driven catalytic system based signal recycling (Fig. 1). In the first step, S1 probe comprising a CD63 aptamer and a muti-"T" section is labeled on the surface of SMBs through avidin and streptomyclophilin interaction to form SMBs-S1 probe; S2–S4 probe complex is composed of three functional section, S2 for EpCAM protein identification, S3 for following chain replacement and S4 for initiation of entropy-driven catalytic system. In the presence of exosomes, CD63 aptamer in S1 sequence and EpCAM aptamer in S2 sequence recognizes corresponding protein on the surface of exosomes and thus generate SMBs-S1-*Exo*-S2-S4 complex (Exo, exosome). After magnet based separation, supernatant containing unbind S2–S4 probe complex was removed. Upon the addition of S5 probe which could hybridize with S3 section, S4 was released from the SMBs-S1-*Exo*-S2-S4 complex. For entropy-driven catalytic system based signal recycling, the released S4 hybridized with toehold region A to form intermediate. The obtained intermediate was unstable and released the strand S6 immediately, leading to exposure nick between S7 and S4 for S8 recognition. Upon the addition of S8 probe, S7 and S4 were displaced from the intermediate. As a result, the fluorescence moiety labeled on S7 which was originally quenched by BHQ-1 reappeared and the S4 triggered a new round of catalysis to generate an amplified signal readout.

2. Results and discussion

2.1. Establishment of SMBs-probe based isolation of exosomes and feasibility of entropy-driven catalytic system based signal recycling

To investigate cooperated identification of target exosome by SMBs-S1 probe and S2–S4 probe complex, we have labeled FAM fluorescence moiety on the terminal of S4 probe. After magnet based separation, the fluorescence signal of FAM in supernatant reflects the formation of SMBs-S1-*Exo*-S2-S4 complex. In the presence of exosomes, FAM fluorescence intensity of unbind S2–S4 probe complex in supernatant was 1765 *a.u.*, which is much higher than that in the absent of exosomes, indicating SMBs-S1 probe and S2–S4 probe complex cooperated in the identification and separation of exosomes (Fig. 2a). Assembly of S6–S7 probe complex was demonstrated through a fluorescence experiment. Before assembly, fluorescence signal of FAM which is labeled on S7 probe was not quenched by BHQ-1 due the long distance between FAM and BHQ-1 blocked FRET effect. From result in Fig. 2b, the fluorescence intensity of assembled S6–S7 probe complex greatly reduced compared with that before assembly. We then verified the S4 triggered entropy-driven catalytic system based signal recycling. Upon the addition of S4 probe, no significant fluorescence signal enhancement appeared compared with assembled S6–S7 probe complex alone, suggesting that addition of S4 could not lead to release of S7 from S6–S7 probe complex. However, FAM signal greatly increased when S8 added in the system (Fig. 2c). Comparison of fluorescence intensity indicates both S4 probe and S8 probe are essential for entropy-driven catalytic system based signal recycling.

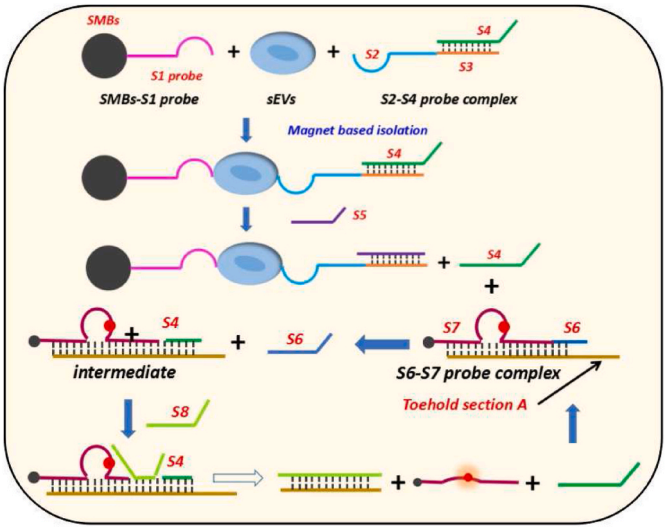

Fig. 1. Working mechanism of the proposed method.

2.2. Optimization of the biosensor for better detection performance

We optimized experimental conditions for a better analytical performance. The concentrations of SMBs-S1 probe and S2–S4 probe complex are critical for accurately identification and quantification of exosomes. Thus, the concentration of SMBs-S1 probe and S2–S4 were firstly optimized. In response to the increasement of SMBs-S1 probe concentration from 50 nM to 200 nM, fluorescence intensity linearly increased. With extra increasement of SMBs-S1 probe concentration, no more obvious enhancements were observed (Fig. 3a). Thus, 200 nM of SMBs-S1 probe was selected for the following experiments. Meanwhile, optimized S2–S4 probe complex concentration was determined to be 100 nM (Fig. 3b). Notably, the concentration ratio of SMBs-S1 probe and S2–S4 probe complex was 1:0.5 which may be attributed to different expression level of CD63 protein and EpCAM protein. With same optimizing protocol, incubation time for exosome isolation was determined 60 min (Fig. 3c). Furthermore, complementary length of S3 and S4 probe was determined 8 nt, which exhibited a highest fluorescence signal enhancements (Fig. S1).

2.3. Analytical performance of dual aptamer recognition-triggered biosensor

The developed dual aptamer recognition-triggered biosensor was utilized for efficient isolation and amplified quantification of exosomes under the optimized experimental conditions. Fig. 4a recorded fluorescence spectrum of the whole sensing system in response to different concentrations of exosomes. The fluorescence intensity increased when exosome concentration raised from 5×10^2 particles/μL to 5×10^6 particles/μL. Calibration curve for quantitative analysis of exosomes concentration is shown in Fig. 4b, in which a good linear relations was obtained between FAM intensity and concentration of exosomes with a correlation coefficient value (R^2) of 0.9973. Moreover, the selectivity of the biosensor was evaluated by analyzing target exosome and recombinant CD63/EpCAM protein. Obviously, the fluorescence intensity of the whole sensing system containing CD63 or EpCAM protein were almost unchanged compared with control group. However, when exosome existed, the fluorescence signal enhanced, indicating that the method could avoid possible interference of free CD63 and EpCAM protein and also the superior selectivity of this biosensor (Fig. 4c). Finally, the potential clinical applications of the dual aptamer recognition-triggered biosensor in complicated biological environments were studied. Exosomes were isolated and quantified by the biosensor in diluted serum samples (spiked exosomes concentration, 2×10^6 particles/μL). Fig. 4d exhibits fluorescence result for exosome detection in 10% blood serum and PBS buffer. Even though, the fluorescence signal in serum was slightly decreased compared with that in PBS buffer, exosome could be quantified without obvious interference, implying favorable accuracy of the proposed biosensor in complex clinical samples. Given all the experimental results above, this biosensor exhibited a favorable exosome detection performance.

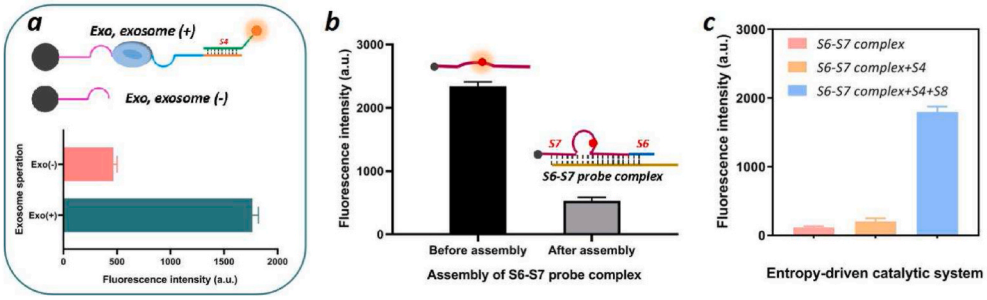

Fig. 2. Investigation of SMBs-probe based isolation of exosomes and feasibility of entropy-driven catalytic system based signal recycling. (a) Fluorescence intensity of the S4 probe when target exosome existed or not; (b) fluorescence intensity of S7 probe before and after the assembly of S6–S7 probe complex; (c) fluorescence intensity of S6–S7 probe complex when incubated with S4 probe and/or with S8 probe.

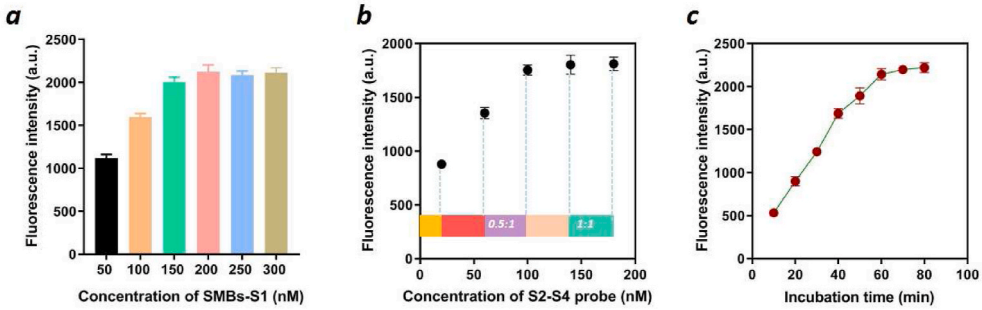

Fig. 3. Optimization of experimental conditions. (a) Fluorescence intensity of the biosensor with different concentration of SMBs-S1 probe; (b) fluorescence intensity of the biosensor with different concentration of S–S4 probe complex; the horizontal column illustrate the concentration ratio of S–S4 probe complex and S1 probe. (c) Fluorescence intensity of the biosensor with different incubation time.

3. Conclusion

In summary, we established a dual aptamer recognition based entropy-driven amplification biosensor for accurate and efficient detection of exosomes. Different from most of former proposed strategies which only detect one exosomal surface protein, such as CD63 or EpCAM, the method exhibited a superior selectivity to target exosome (Table 1). Given the possible interference from cell debris, free EpCAM and CD63 protein in serum environment, methods with only one exosomal surface protein as recognition target will be easily affected and output false positive results. Furthermore, the biosensor also showed a favorable detection stability even in complicated environments. Besides the high accuracy and stability, the method also has the advantages of high sensitivity. Entropy-driven catalytic system based signal recycling provided efficient signal amplification without using enzymes, and could be extended to a versatile platform for diverse exosomes screening. This accurate and effective biosensor could be further applied to detect other biologically relevant molecules, holding potential promise for early diagnosis and treatment of diseases.

4. Experimental

4.1. Materials and apparatus

The DNA sequences for exosome isolation and for entropy-driven amplification were designed according to former references [18,21,25] and are listed in Table S1. DNA sequences were synthesized by Sangon Biotech Co., Ltd. (Shanghai, China). The obtained DNA sequences were purified by high-performance liquid chromatography. SMBs were purchased from Sigma-Aldrich (Shanghai, China). Human serum samples were purchased from Solarbio. The fluorescence spectra were detected by a Hitachi F-7100 fluorescence spectrophotometer (Beijing, China). For FAM detection, the excitation wavelength was 492 nm and the emission wavelength was 500 nm–700 nm. The fluorescence intensities of 515 nm were utilized for comparison and curve fitting.

4.2. Assembly of SMBs-S1 probe and S2–S4 probe complex

Assembly of S2–S4 probe complex complex was performed according to the following protocol: 5 μL S2 probe, 5 μL S3 probe and 5 μL S4 probe were mixed in a tube and diluted by PBS butter to 2 μM. The mixture were then heated to 90 °C for 10 min and cooled to room temperature in 2 h. Assembly of SMBs-S1 probe was conducted according to the instruction of SMBs. In brief, wash of obtained SMBs by 1 × B&W buffer solution (10 mM Tris-HCl, pH, 7.5, 1 mM EDTA, 2.0 M NaCl) for three times and then was diluted to 50 μg/ml; the result SMBs was then incubated with S1 probe (10 mM) for 20 min; unbind S1 probe was removed after magnet based separation.

4.3. Assembly of S6–S7 probe complex and validation of the entropy-driven amplification

Assembly of S6–S7 probe complex was performed according to the following protocol: 5 μL S6 probe, 5 μL S7 probe and 5 μL ssDNA template probe were mixed in a tube and diluted by PBS butter to 2 μM. The mixture were then heated to 90 °C for 10 min and cooled to room temperature in 2 h. The fluorescence signals of S6 probe before and after assembly were detected by Hitachi F-7100 fluorescence spectrophotometer (Beijing, China).

Synthesized S4 probe was utilized for the validation of the entropy-driven amplification. The whole amplification process was performed in PBS buffer solutions (20 mM) containing 5 mM $Mg(Ac)_2$. 5 μL S6–S7 probe complex (2 μM) was incubated with 5 μL Synthesized S4 probe and 5 μL S8 probe for 1 h at 30 °C. The fluorescence signals of S6 probe before and after assembly were detected by Hitachi F-7100 fluorescence spectrophotometer (Beijing, China). Study the role of S8 probe in the

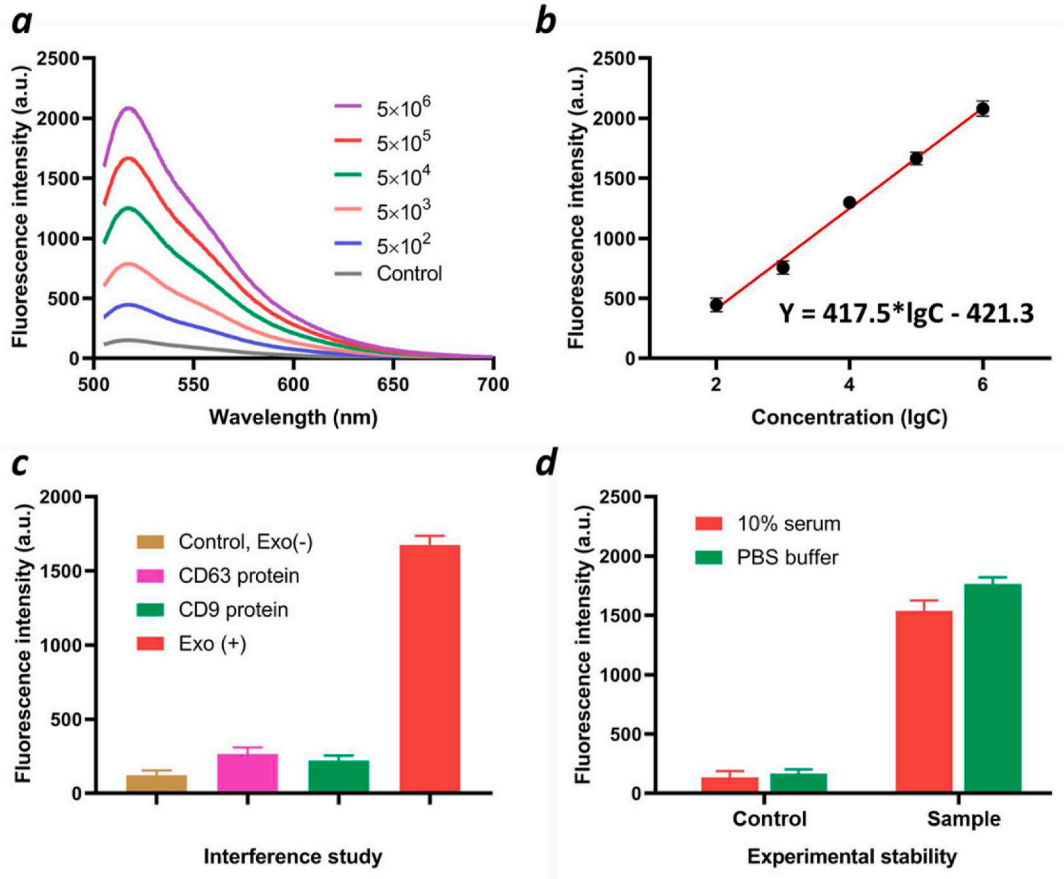

Fig. 4. Detection performance of the proposed method. (a) Fluorescence spectrum of the biosensor when detecting different concentration of exosomes; (b) correlation equation between the obtained fluorescence intensity and the concentration exosome; (c) fluorescence intensity of the biosensor when detecting CD63 protein, EpCAM protein and target exosome; (d) fluorescence intensity of the biosensor in complicated experimental conditions.

Table 1
Comparison of exosome detection methods.

Tittle	Principle	Sensitivity (particles/μL)	Target	Interference	Wash-free	Ref
The strategy	entropy-driven amplification	10^2	CD63+EpCAM	No	No	
CRISPR-Cas12a	*Trans*-cleavage	10^2	CD63	Yes	No	[22]
AcmPLA	RCA	10^2	CD63+bio-layer	No	No	[18]
AID-Cas	Dual amplification	10^2	CD63	Yes	Yes	[21]

RCA, rolling circle amplification.

entropy-driven amplification was performed followed the protocol: 5 μL S6–S7 probe complex (2 μM) was incubated with 5 μL Synthesized S4 probe.

4.4. Detection performance of exosomes

The procedures of incubating A547 cell and isolating exosomes were from related references. In brief, exosomes were isolated from cell supernatant and isolated by ultra-high speed centrifugation. Extracted exosomes were quantified by Particle Metrix Zetaview Nanoparticle Tracking Analysis (Beijing, China) and then diluted to different concentrations. The 10 μL obtained exosomes were mixed with 10 μL SMBs-S1 probe and 10 μL S2–S4 probe complex. The mixture was incubated at 30 °C for 40 min and then washed by PBS buffer for three times after magnet based separation. Afterwards, the sediment was re-suspended by 100 μL PBS buffer and incubated with 10 μL S5 probe for 20 min. After magnet based separation, supernatant containing S4 probe was utilized for the entropy-driven amplification following the above protocol in 4.3.

CRediT authorship contribution statement

Chengxiang Yu: designed the method, Writing – original draft, performed experiments and wrote the manuscript. **Lei Li:** cooperated in experiments. **Lehong Liu:** Data curation, assisted data processing and revision of the manuscript. **Zhongping Wang:** Data curation, assisted data processing and revision of the manuscript. **Jianhua Zhu:** Project administration, Funding acquisition, designed and funded the project, and also the revision of manuscript.

Acknowledgments

Notes: The authors declare no competing financial interest.

Appendix A. Supplementary data

Supplementary data to this article can be found online at https://doi.org/10.1016/j.ab.2021.114433.

References

[1] M. Karatas, B. Zengel, R. Durusoy, F. Tasli, Z. Adibelli, C. Simsek, A. Uslu, Medicine (Baltim.) 100 (2021), e24164.
[2] T. Tamura, Y. Yoshioka, S. Sakamoto, T. Ichikawa, T. Ochiya, Int. J. Mol. Sci. (2020) 21.
[3] M. Yang, C. Liu, X. Yu, Discov. Med. 27 (2019) 211–220.
[4] J.J. Yin, C.B. Pollock, K. Kelly, Cell Res. 15 (2005) 57–62.
[5] N. Brook, E. Brook, A. Dharmarajan, C.R. Dass, A. Chan, Int. J. Biochem. Cell Biol. 96 (2018) 63–78.
[6] F. Salvador, A. Llorente, R.R. Gomis, J. Pathol. 249 (2019) 6–18.
[7] X. Yuan, N. Qian, S. Ling, Y. Li, W. Sun, J. Li, R. Du, G. Zhong, C. Liu, G. Yu, D. Cao, Z. Liu, Y. Wang, Z. Qi, Y. Yao, F. Wang, J. Liu, S. Hao, X. Jin, Y. Zhao, J. Xue, D. Zhao, X. Gao, S. Liang, Y. Li, J. Song, S. Yu, Y. Li, Theranostics 11 (2021) 1429–1445.
[8] M. Ono, N. Kosaka, N. Tominaga, Y. Yoshioka, F. Takeshita, R.U. Takahashi, M. Yoshida, H. Tsuda, K. Tamura, T. Ochiya, Sci. Signal. 7 (2014) ra63.
[9] G.L. Wong, S. Abu Jalboush, H.W. Lo, Cancers 12 (2020).
[10] S.W. Wen, J. Sceneay, L.G. Lima, C.S. Wong, M. Becker, S. Krumeich, R.J. Lobb, V. Castillo, K.N. Wong, S. Ellis, B.S. Parker, A. Moller, Cancer Res. 76 (2016) 6816–6827.
[11] K. Tiedemann, G. Sadvakassova, N. Mikolajewicz, M. Juhas, Z. Sabirova, S. Tabaries, J. Gettemans, P.M. Siegel, S.V. Komarova, Transl Oncol 12 (2019) 462–474.
[12] S. Lin, Z. Yu, D. Chen, Z. Wang, J. Miao, Q. Li, D. Zhang, J. Song, D. Cui, Small 16 (2020), e1903916.
[13] F. Yang, X. Liao, Y. Tian, G. Li, Biotechnol. J. (2017) 12.
[14] P. Zhang, X. Zhou, M. He, Y. Shang, A.L. Tetlow, A.K. Godwin, Y. Zeng, Nat Biomed Eng 3 (2019) 438–451.
[15] A. Bagheri Hashkavayi, B.S. Cha, E.S. Lee, S. Kim, K.S. Park, Anal. Chem. 92 (2020) 12733–12740.
[16] S. Khodashenas, S. Khalili, M. Forouzandeh Moghadam, Biotechnol. Lett. 41 (2019) 523–531.
[17] Y. Zhang, J. Jiao, Y. Wei, D. Wang, C. Yang, Z. Xu, Anal. Chem. 92 (2020) 15244–15252.
[18] X. Zhao, C. Luo, Q. Mei, H. Zhang, W. Zhang, D. Su, W. Fu, Y. Luo, Anal. Chem. 92 (2020) 5411–5418.
[19] Y. Pan, L. Wang, Y. Deng, M. Wang, Y. Peng, J. Yang, G. Li, Chem Commun (Camb) 56 (2020) 13768–13771.
[20] Y. Yu, W.S. Zhang, Y. Guo, H. Peng, M. Zhu, D. Miao, G. Su, Biosens. Bioelectron. 167 (2020) 112482.
[21] X. Zhao, L. Zeng, Q. Mei, Y. Luo, ACS Sens. 5 (2020) 2239–2246.
[22] X. Zhao, W. Zhang, X. Qiu, Q. Mei, Y. Luo, W. Fu, Anal. Bioanal. Chem. 412 (2020) 601–609.
[23] X. Chen, M. Jia, L. Liu, X. Qiu, H. Zhang, X. Yu, W. Gu, G. Qing, Q. Li, X. Hu, R. Wang, X. Zhao, L. Zhang, X. Wang, C. Durkan, N. Wang, G. Wang, Y. Luo, Small 16 (2020), e2002800.
[24] D. Jin, F. Yang, Y. Zhang, L. Liu, Y. Zhou, F. Wang, G.J. Zhang, Anal. Chem. 90 (2018) 14402–14411.
[25] G.Z. Zhang L., J. Tong, X. Zhao, J. Ren, Microchem. J. 158 (2020), 105239.